

High-Performance Microstructure Core Photonic Crystal Fibre-Based Biosensor for Alcohol Detection

Ang Chuan Shi¹, Abdul Mu'iz Maida¹, Nianyu Zou², and Feroza Begum^{1, *}

Abstract—A high-performance photonic crystal fibre-based alcohol biosensor is introduced for the selective test analytes: propanol, butanol, and pentanol operating at wavelengths ranging from 0.8 to 2.0 μm . The performance of the proposed sensor with the architecture of octagonal-shaped cladding air holes in two rings surrounding a single infiltrated hexagonal core hole produces high relative sensitivities, low confinement losses, small effective areas, and high nonlinear coefficients. At the optimal 1.4 μm wavelength, propanol, butanol, and pentanol assessed relative sensitivities of 93.10%, 93.95%, and 94.70%, respectively, and confinement losses of 6.38×10^{-10} dB/m for propanol, 2.12×10^{-10} dB/m for butanol and 1.04×10^{-10} dB/m for pentanol. Moreover, the nonlinear coefficients achieved results of $2446 \text{ W}^{-1}\text{km}^{-1}$ for propanol, $2703 \text{ W}^{-1}\text{km}^{-1}$ for butanol, and $2869 \text{ W}^{-1}\text{km}^{-1}$ for pentanol, at the optimum wavelength. These outstanding results of optical properties prove the potential and capabilities for practical sensing and optical communication applications.

1. INTRODUCTION

Photonic Crystal Fibres (PCFs) have gained increased popularity over the last two decades due to their physical properties and their implementation in various fields ranging from data transfer to sensing applications [1]. Additionally, PCFs are widely studied due to their design flexibility, superior light confinement, compact size, and broad birefringent adjustments [2]. The accuracy and reliability can also be altered or improved by varying the values of pitch and air hole diameter, and modifying the number of rings [2]. In comparison to Conventional Optical Fibres (COFs), PCFs have larger refractive indices between the cladding and the core. Hence, the evanescent field can be easily controlled in PCFs [3]. PCFs have evolved over the years taking many shapes and sizes in terms of their cladding and core designs depending on the requirements. Some cladding lattices include hexagonal [4], octagonal [5], square [6], and circular [7] designs, whereas the air hole shapes have been in the form of circle [8], ellipse [9], square [10], and many more. Furthermore, there have also been multiple variations in the core design, particularly a hollow core. The common shapes incorporate circular [11], elliptical [12], and square [13] geometries.

In recent years, various alcohol detecting PCF sensors have been introduced by different groups of researchers focusing on selective test analytes: propanol, butanol, and pentanol. Vishwakarma et al. [14] recommended a PCF of 6 circular cladding air hole rings and a single pentanol-infiltrated circular core hole. This study did not record values of relative sensitivity but obtained confinement losses of around 10^{-2} dB/m over the specified operating wavelength of 1.4 μm . Similarly, a group of researchers [15] proposed an identical fibre design that comprised 6 dodecagonal lattice cladding air holes and 1 circular core hole with infiltration of propanol and butanol. At 1.4 μm operating wavelength, the fibre design has deduced confinement losses of about 10^{-2} dB/m for both analytes, and

Received 12 May 2022, Accepted 23 September 2022, Scheduled 13 October 2022

* Corresponding author: Feroza Begum (feroza.begum@ubd.edu.bn).

¹ Faculty of Integrated Technologies, Universiti Brunei Darussalam, Jalan Tungku Link, Gadong, Bandar Seri Begawan BE1410, Brunei. ² Research Institute of Photonics, Dalian Polytechnic University, Dalian 116034, China.

no relative sensitivity has been recorded. As these studies did not assess values of relative sensitivity, the design cannot be evaluated for sensing applications. Additionally, Asaduzzaman et al. [16] brought forward a PCF sensor with a circular lattice cladding of 3 layers with the intricate core structure of 11 hollow holes arranged in a hexagonal manner for propanol detection. This complex design recorded low confinement losses of the order of 10^{-11} dB/m, however, reported underwhelming relative sensitivity results of 37.54% at an operating wavelength of 1.4 μm . Despite a complex fibre design, the sensor has displayed extremely low relative sensitivity to the analyte and may cause difficulty in fabrication due to the number of holes of different dimensions. On the contrary, a different group of researchers [17] had recently implemented a hollow-core photonic crystal fibre for sensing propanol and butanol. The cladding area has a 5 layer of circular air holes in a hexagonal mesh, while the core includes a single large circular hollow hole. It boasted a high relative sensitivity of 86.74% for propanol and 88.34% for butanol, at the optimum wavelength of 1.4 μm . On the other hand, the confinement losses were noted to be about 10^{-10} dB/m to 10^{-11} dB/m for these test analytes. The large core hole allows high interaction between the light signal and the alcohol analytes, but applying numerous cladding holes causes a disadvantage in the fabrication process. Then, Ahmed et al. [18] recommended a Surface Plasmon Resonance (SPR)-based PCF sensor to analyse three different alcohols: propanol, butanol, and pentanol. The designed structure consists of a cladding region with 17 air holes arranged in an 'X' pattern and a core region of a large continuous circular ring positioned exterior to the cladding. Their proposed PCF was performed to obtain relative sensitivities for propanol, butanol, and pentanol of 41.29%, 41.30%, and 41.32%, respectively, at a 1.5 μm operating wavelength. The study is a novel method for alcohol sensors; however, the presented results are very low, and the application in practical use is uncertain. Another approach was undertaken by Paul et al. [19], whereby a porous cored octagonal PCF was proposed. The researchers have introduced 5 circular air hole rings in an octagonal lattice that encircles a core region with 2 circular rings. With this architecture, they managed to depict moderate results of relative sensitivities and confinement losses. At the wavelength of 1.4 μm , propanol managed to obtain relative sensitivity of 69.14%, 69.92% for butanol, and 70.09% for pentanol. Confinement losses were found in the order of 10^{-10} dB/m for propanol, 10^{-11} dB/m for butanol, and 10^{-12} dB/m for pentanol. Due to the vast design, there shall be complications in manufacturing such a fibre structure and prone to deviation from the specified dimensions. Furthermore, Ahmed et al. [20] presented an alcohol PCF sensor of two different core designs, while maintaining the cladding design constant as part of their study. The two different core designs are 19 circular hollow holes and 19 elliptical hollow holes. The former design recorded achieving better relative sensitivities of 65.95%, 66.35%, and 66.73% for propanol, butanol, and pentanol, respectively, whereas confinement losses of about 10^{-10} dB/m for all the alcohols. However, the latter design depicted relative sensitivities of 58.17% for propanol, 58.74% for butanol, and 59.29% for pentanol, and confinements losses of orders 10^{-10} dB/m. These datasets are obtained at the optimum wavelength of 1.5 μm . By including many hollow holes in both designs, fabrication issues shall prevail, and results of optical parameters may vary tremendously from recorded data.

From the literature [14–20], this research study has implemented a simple fibre design for alcohol detection of the selective test analytes: propanol, butanol, and pentanol. The simple architecture includes a single injected hexagon-shaped core hole and 2 layers of octagonal cladding air holes positioned in a hexagonal lattice, which outlines high relative sensitivities and low confinement losses at the optimal wavelength.

2. DESIGN

A total diameter of 20.05 μm PCF has been proposed, which utilises a hollow core structure. The design includes 3 primary components: core, cladding, and Perfectly Matched Layer (PML). The PML is the outermost layer of the fibre specified to be 10% of the overall size of the optical fibre, which operates as a medium to prevent light from reflecting into the cladding region through absorption. The cladding area consists of two rings of octagonal-shaped air holes arranged in a hexagonal configuration. These air holes allow the confinement of light in the core by the high contrast in the refractive index that ultimately improves the sensitivity of the PCF in analysing the selected test analytes. Lastly, the core is composed of a solo hexagon-shaped hollow hole for analyte infiltration.

The cladding air holes are separated by a pitch length, the distance between centres of adjacent cladding air holes, of 2.954 μm . In Figure 1, the architecture of the proposed alcohol PCF sensor is illustrated. The cladding air holes are closely packed due to their high value of Air-Filling Fraction (AFF) of 0.96. AFF is the ratio of the air hole length to pitch distance. The hexagonal core hole has a side-to-side length d_a of 2.836 μm , and the dimension of the octagon cladding holes is specified to a similar size of 2.836 μm . The background material is fused silica.

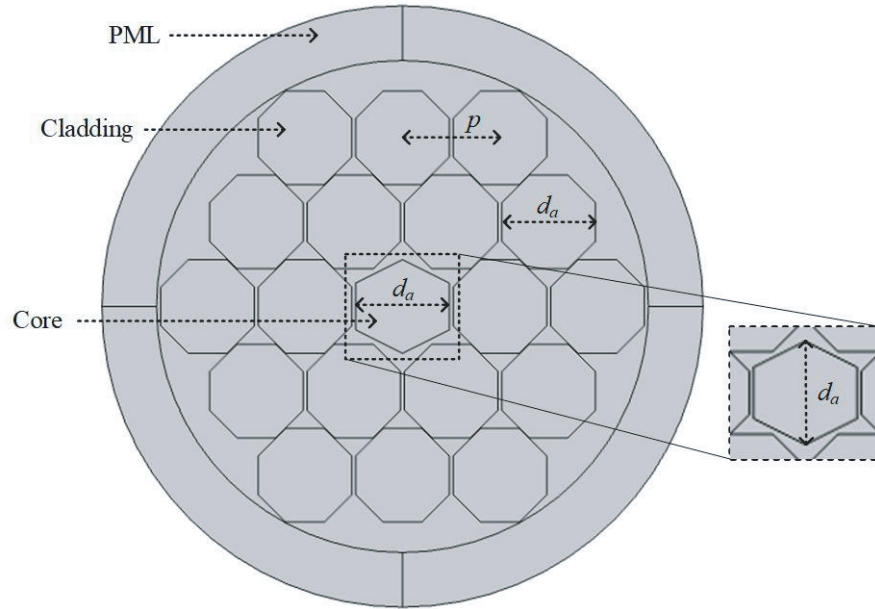


Figure 1. The architecture of the proposed alcohol sensor.

3. METHODOLOGY

Each variable in the proposed PCF was investigated using the COMSOL Multiphysics version 5.6 software, based on the full Finite Vector Finite Element Method (FV-FEM) approach. From the derivation of Maxwell’s equation, this technique was utilised to create mesh analysis that resulted in 17,297 mesh vertices, 34,472 triangular elements, and 2,829 edge elements, among other elements.

Three selective analytes were evaluated as part of the study: propanol, butanol, and pentanol. A set of operating wavelengths ranging from 0.8 to 2.0 μm was employed for all three test analytes. Figure 2 shows the refractive indices of propanol, butanol, and pentanol with respect to the specified operating wavelength.

To determine the reliability and effectiveness of the proposed fibre, 6 parameters were considered: effective refractive index, power fraction, relative sensitivity, confinement loss, effective area, and nonlinear coefficient.

The effective refractive index n_{eff} of silica background material and alcohol-infiltrated core hole can be obtained by [21]:

$$n_{\text{eff}}(\lambda) = \sqrt{1 + \frac{A_1\lambda^2}{\lambda^2 - B_1} + \frac{A_2\lambda^2}{\lambda^2 - B_2} + \frac{A_3\lambda^2}{\lambda^2 - B_3}} \quad (1)$$

where λ is the operating wavelength, $A_{(i=1,2,3)}$, and $B_{(i=1,2,3)}$ are coefficients of that material.

Power fraction F is the quantification of power flowing in the core against the total fibre area and

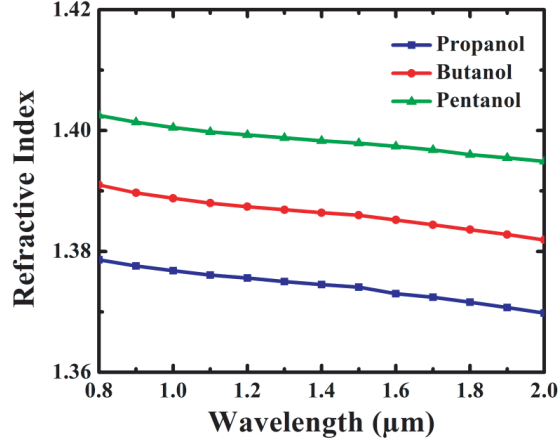


Figure 2. Refractive index for propanol, butanol and pentanol with respect to wavelength.

is defined by [22–24]:

$$F = \frac{(sample) \int \text{Re} (E_x H_y - E_y H_x) dx dy}{(total) \int \text{Re} (E_x H_y - E_y H_x) dx dy} \times 100 \quad (2)$$

where E_x , E_y and H_x , H_y are the transverse electric field and magnetic field in the x - and y -planes, respectively.

Relative sensitivity R represents the interaction between light and test analyte to be sensed, which can be expressed as [24–26]:

$$R = \frac{n_r}{n_{\text{eff}}} \times F \quad (3)$$

where n_r is the refractive index of the test analytes: propanol, butanol, and pentanol.

Confinement loss L can be calculated from the evaluated effective refractive index and determines the amount of light leakage. It can be quantified by [27, 28]:

$$L = \frac{40\pi}{\ln(10)\lambda} \text{Im} [n_{\text{eff}}] \times 10^6 \quad (4)$$

where $\text{Im}(n_{\text{eff}})$ is the imaginary part of the effective mode index.

Effective area A_{eff} represents the cross-sectional area of the PCF in transverse dimensions covered by the Gaussian profile of fundamental mode of light and is computed by [29–33]:

$$A_{\text{eff}} = \frac{\left(\int_{-\infty}^{\infty} \int_{-\infty}^{\infty} |E|^2 dx dy \right)^2}{\int_{-\infty}^{\infty} \int_{-\infty}^{\infty} |E|^4 dx dy} \quad (5)$$

where E is the transverse electric fields of the guided mode.

The nonlinear coefficient demonstrates the nonlinearity of light interaction with the optical material and is found by [32, 34–36]:

$$\gamma = \left(\frac{2\pi}{\lambda} \right) \left(\frac{n_2}{A_{\text{eff}}} \right) \quad (6)$$

where n_2 is the nonlinear refractive index.

4. RESULTS AND DISCUSSION

The proposed PCF has been simulated to deduce the numerical values of effective refractive index, power fraction, relative sensitivity, confinement loss, effective area, and nonlinear coefficient. The distribution of the electric fields when propagating light interacts with the alcohol analytes is shown in Figure 3. As can be seen, the light is confined completely within the core region of the fibre at a wavelength of 1.4 μm .

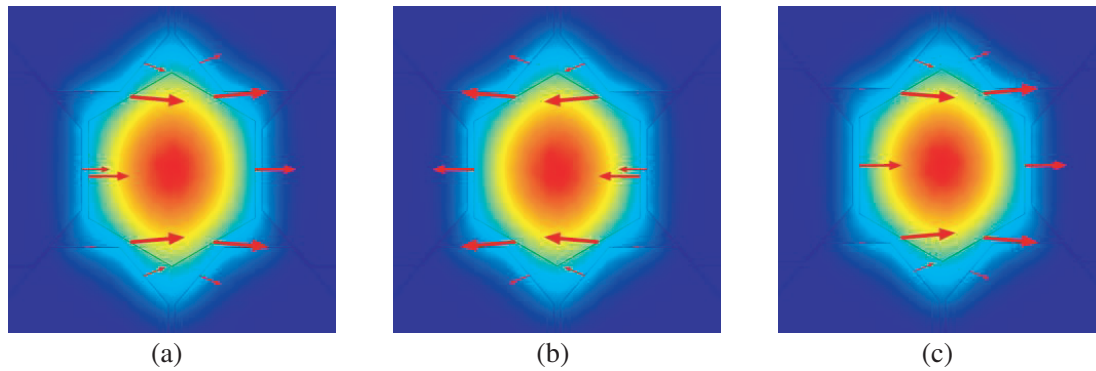


Figure 3. Electric field distribution profile of (a) propanol, (b) butanol and (c) pentanol for the proposed PCF at optimum wavelength of 1.4 μm .

To distinguish between the analytes of propanol, butanol, and pentanol, refractive indices are used that are unique to each of them. The combination of the refractive indices of the analytes and the background material provides the effective refractive indices through the simulation. Figure 4 displays the relationship between effective refractive index and wavelength; the effective refractive index decreases gradually as wavelength increases. This tendency arises from the theoretical behaviour of light signals that are highly confined at higher refractive indices. Moreover, it can be noted that pentanol possesses a higher refractive index than butanol and pentanol.

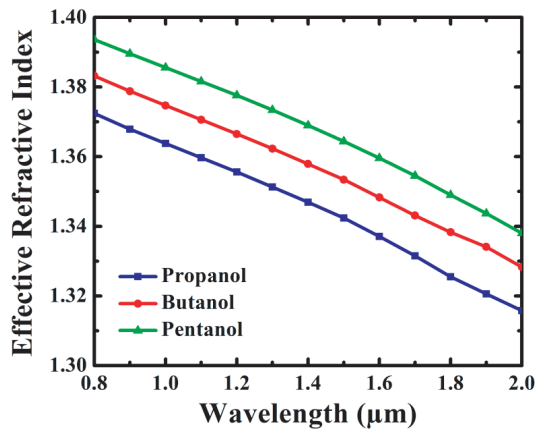


Figure 4. Effective refractive index results for propanol, butanol and pentanol of the proposed PCF over the range of operating wavelengths.

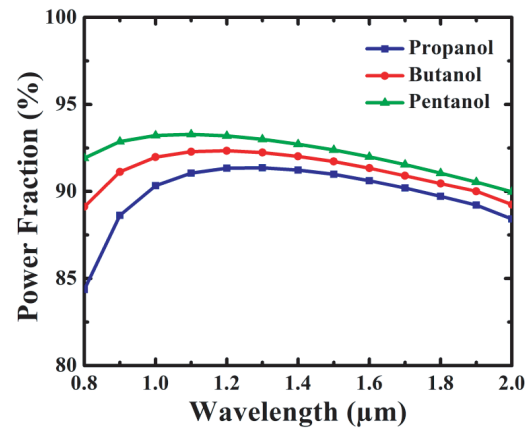


Figure 5. Power fraction results for propanol, butanol and pentanol of the proposed PCF over the range of operating wavelengths.

The power ratio transmitting through the PCF resulted in excellent set of data where the test analytes obtained more than 90% at 1.4 μm , shown in Figure 5. The graph demonstrates that propanol, butanol, and pentanol initially increase at lower wavelengths and then subsequently decrease as the

operating wavelength increases to 2.0 μm . The power fraction measures the amount of power flowing in the core versus the total fibre region. Maximum power is reached as wavelength increases to optimal wavelength value and sequentially decreases as wavelength increases further. The optimum wavelength is marked at 1.4 μm , which deduced power fractions of propanol to be 91.23%, 92.01% for butanol, and 92.72% for pentanol.

Figure 6 represents the relative sensitivities of the test analytes in the proposed PCF against operating wavelengths from 0.8 to 2.0 μm . The relative sensitivity increases initially at earlier wavelength until 1.4 μm and declines gradually as the wavelength further increases to 2.0 μm . In the figure, the maximum relative sensitivities obtained at the operating wavelength of 1.4 μm were 93.10%, 93.95%, and 94.70%, for propanol, butanol, and pentanol, respectively.

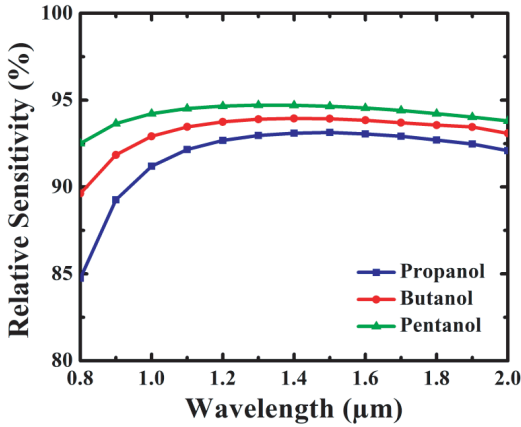


Figure 6. Relative sensitivity results for propanol, butanol and pentanol of the proposed PCF over the range of operating wavelengths.

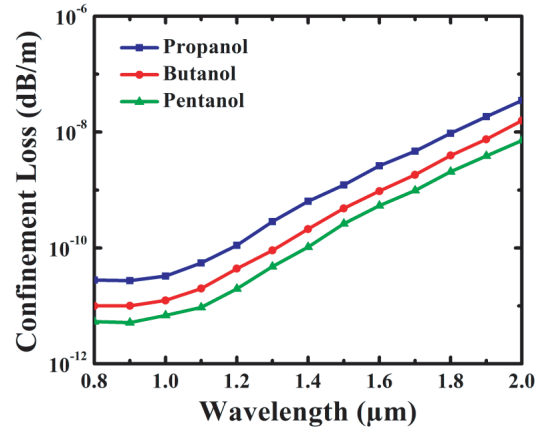


Figure 7. Confinement loss results for propanol, butanol and pentanol of the proposed PCF over the range of operating wavelengths.

The simulated PCF produces low confinement losses due to the cladding design and its characteristics. Figure 7 displays the confinement losses of propanol, butanol, and pentanol with respect to operating wavelength for the proposed PCF. By referring to the figure, it is apparent that the confinement loss increases as the wavelength increases. This performance appears because the leakage of light intensifies as wavelength increases. The confinement losses are found in the order of 10^{-11} to 10^{-12} dB/m, specifically at an optimal wavelength of 1.4 μm , about 6.38×10^{-10} dB/m for propanol, 2.12×10^{-10} dB/m for butanol, and 1.04×10^{-10} dB/m for pentanol.

The relationship between analyte effective area and operating wavelength for the proposed PCF is presented in Figure 8. The effective area increases exponentially as wavelength increases from 0.8 μm to 2.0 μm for all the selective alcohol analytes. As the effective area depends on the intensity of the light and propagating electric fields, the fields in the cross-sectional area increase with wavelength. A similar trend is proven in Figure 8. With the specified 1.4 μm optimum wavelength, the effective area is evaluated to 0.0587 μm^2 , 0.0531 μm^2 , and 0.0501 μm^2 for propanol, butanol, and pentanol, respectively.

Due to the opposing nature between the nonlinear coefficient and effective area, the coefficient decreases exponentially as wavelength increases. Figure 9 illustrates the nonlinearity of the proposed PCF from propanol, butanol, and pentanol against operating wavelength. At 1.4 μm operating wavelength, the nonlinear coefficients are recorded for propanol, butanol, and pentanol to be $2446 \text{ W}^{-1}\text{km}^{-1}$, $2703 \text{ W}^{-1}\text{km}^{-1}$, and $2869 \text{ W}^{-1}\text{km}^{-1}$, respectively.

To date, there are various researches for detecting alcohols via the implementation of photonic crystal fibers. Table 1 presents the comparison of previous researches to the proposed PCF which involves propanol, butanol, and pentanol. It can be noted that both relative sensitivities and confinement losses of the proposed PCF demonstrate better results.

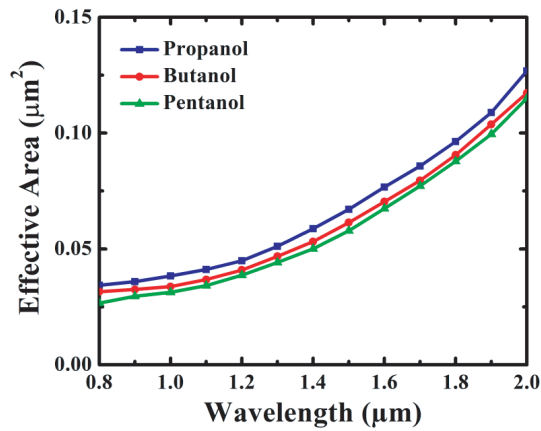


Figure 8. Effective area results for propanol, butanol and pentanol of the proposed PCF over the range of operating wavelengths.

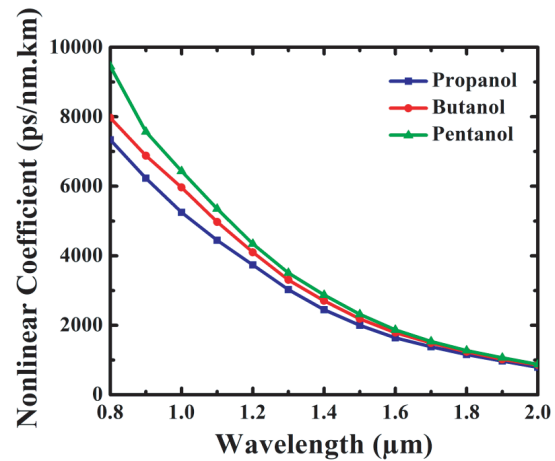


Figure 9. Nonlinear coefficient results for propanol, butanol and pentanol of the proposed PCF over the range of operating wavelengths.

Table 1. Performance table of proposed PCF compared to previous PCFs.

	Wavelength (μm)	Analyte	Relative Sensitivity (%)	Confinement Loss (dB/m)
Ref. [14]	1.4	Pentanol	-	$\sim 10^{-2}$
Ref. [15]	1.4	Propanol Butanol	-	$\sim 10^{-2}$ 10^{-2}
Ref. [16]	1.4	Propanol	37.54	$\sim 10^{-11}$
Ref. [17]	1.4	Propanol Butanol	86.74 88.34	$\sim 10^{-10}$ $\sim 10^{-11}$
Ref. [18]	1.5	Propanol Butanol Pentanol	41.29 41.30 41.32	-
Ref. [19]	1.4	Propanol Butanol Pentanol	69.14 69.92 70.09	$\sim 10^{-10}$ $\sim 10^{-11}$ $\sim 10^{-12}$
Ref. [20]	1.5	Propanol Butanol Pentanol	65.95 66.35 66.73	$\sim 10^{-10}$ $\sim 10^{-10}$ $\sim 10^{-11}$
Ref. [20]	1.55	Propanol Butanol Pentanol	58.17 58.74 59.29	$\sim 10^{-10}$ $\sim 10^{-11}$ $\sim 10^{-10}$
Proposed PCF	1.4	Propanol Butanol Pentanol	93.10 93.95 94.70	$\sim 10^{-10}$ $\sim 10^{-10}$ $\sim 10^{-10}$

5. CONCLUSION

A high-performance PCF biosensor for alcohol sensing has been proposed with low confinement losses. The architectural design for the biosensor consists of 1 hexagonal core hole infiltrated with propanol, butanol, and pentanol, and 18 octagonal cladding air holes in 2 rings arranged in a hexagonal lattice. By allowing a simple design, there shall be easy fabrication and restricted derivation from defined hole dimensions. This fibre structure manages to obtain relative sensitivities over 93%: 93.10% for propanol, 93.95% for butanol, and 94.70% for pentanol, at the operating wavelength of 1.4 μm . Moreover, partially complete light confinement in the core was achieved, which obtained confinement losses in the order of 10^{-10} dB/m for all alcohol analytes. Other optical parameters of effective area and nonlinear coefficient have also been determined. Thus, the fibre design is not limited to sensing applications but can be additionally applied to optical communications for supercontinuum generation because of the high nonlinear coefficient.

REFERENCES

1. Rashed, A. N. Z., M. S. F. Tabbour, and P. Vijayakumari, "Numerical analysis of optical properties using octagonal shaped photonic crystal fiber," *J. Opt. Commun.*, 2019.
2. Mahfuz, M. Al., M. A. Mollah, M. R. Momota, A. K. Paul, A. Masud, S. Akter, and M. R. Hasan, "Highly sensitive photonic crystal fiber plasmonic biosensor: Design and analysis," *Opt. Mater. (Amst.)*, Vol. 90, 315–321, 2019.
3. Rifat, A. A., M. R. Hasan, R. Ahmed, and H. Butt, "Photonic crystal fiber-based plasmonic biosensor with external sensing approach," *J. Nanophotonics*, Vol. 12, No. 1, 012503, 2017.
4. Islam, M. S., J. Sultana, M. Faisal, M. R. Islam, A. Dinovitser, B. W.-H. Ng, and D. Abbott, "A modified hexagonal photonic crystal fiber for terahertz applications," *Opt. Mater. (Amst.)*, Vol. 79, 336–339, 2018.
5. Ahmed, K., M. Morshed, S. Asaduzzaman, and M. F. H. Arif, "Optimization and enhancement of liquid analyte sensing performance based on square-cored octagonal photonic crystal fiber," *Optik (Stuttg.)*, Vol. 131, 687–696, 2017.
6. Cordeiro, C. M. B., A. K. L. Ng, and H. Ebendorff-Heidepriem, "Ultra-simplified single-step fabrication of microstructured optical fiber," *Sci. Rep.*, Vol. 10, No. 1, 9678, 2020.
7. Dhanu Krishna, G., G. Prasannan, S. K. Sudheer, and V. P. Mahadevan Pillai, "Analysis of zero dispersion shift and supercontinuum generation at near IR in circular photonic crystal fibers," *Optik (Stuttg.)*, Vol. 145, 599–607, 2017.
8. Zhang, H., X. Zhang, H. Li, Y. Deng, X. Zhang, L. Xi, X. Tang, and W. Zhang, "A design strategy of the circular photonic crystal fiber supporting good quality orbital angular momentum mode transmission," *Opt. Commun.*, Vol. 397, 59–66, 2017.
9. Ahmed, K., B. K. Paul, B. Vasudevan, A. N. Z. Rashed, R. Maheswar, I. S. Amiri, and P. Yupapin, "Design of D-shaped elliptical core photonic crystal fiber for blood plasma cell sensing application," *Results Phys.*, Vol. 12, 2021–2025, 2019.
10. Medjouri, A., L. M. Simohamed, O. Ziane, and A. Boudrioua, "Investigation of high birefringence and chromatic dispersion management in photonic crystal fibre with square air holes," *Optik (Stuttg.)*, Vol. 126, No. 20, 2269–2274, 2015.
11. Hassan, M. M., M. A. Kabir, M. N. Hossain, T. K. Nguyen, B. K. Paul, K. Ahmed, and V. Dhasarathan, "Numerical analysis of circular core shaped photonic crystal fiber for orbital angular momentum with efficient transmission," *Appl. Phys. B*, Vol. 126, No. 9, 145, 2020.
12. Sultana, J., M. S. Islam, M. Faisal, M. R. Islam, B. W.-H. Ng, H. Ebendorff-Heidepriem, and D. Abbott, "Highly birefringent elliptical core photonic crystal fiber for terahertz application," *Opt. Commun.*, Vol. 407, 92–96, 2018.
13. Jibon, R. H., M. Ahmed, M. E. Rahaman, M. K. Hasan, M. M. Shaikh, and A. Tooshil, "Nicotine sensing by photonic crystal fiber in THz regime," *2021 2nd International Conference on Robotics, Electrical and Signal Processing Techniques (ICREST)*, 334–337, IEEE, 2021.

14. Vishwakarma, R., P. Kumar, S. Saha, G. Rout, and J. S. Roy, "Zero dispersion photonic crystal fibers for nonlinear applications," *2017 8th International Conference on Computing, Communication and Networking Technologies (ICCCNT)*, 1–4, IEEE, 2017.
15. Kumar, P., Rohan, V. Kumar, and J. S. Roy, "Dodecagonal photonic crystal fibers with negative dispersion and low confinement loss," *Optik (Stuttg.)*, Vol. 144, 363–369, 2017.
16. Asaduzzaman, S., M. F. H. Arif, K. Ahmed, and P. Dhar, "Highly sensitive simple structure circular photonic crystal fiber based chemical sensor," *2015 IEEE International WIE Conference on Electrical and Computer Engineering (WIECON-ECE)*, 151–154, IEEE, 2015.
17. Habib, M. A., M. S. Anower, A. AlGhamdi, O. S. Faragallah, M. M. A. Eid, and A. N. Z. Rashed, "Efficient way for detection of alcohols using hollow core photonic crystal fiber sensor," *Opt. Rev.*, Vol. 28, No. 4, 383–392, 2021.
18. Ahmed, K., M. J. Haque, M. A. Jabin, B. K. Paul, I. S. Amiri, and P. Yupapin, "Tetra-core surface plasmon resonance based biosensor for alcohol sensing," *Phys. B Condens. Matter*, Vol. 570, 48–52, 2019.
19. Paul, B. K., M. S. Islam, K. Ahmed, and S. Asaduzzaman, "Alcohol sensing over O+E+S+C+L+U transmission band based on porous cored octagonal photonic crystal fiber," *Photonic Sensors*, Vol. 7, No. 2, 123–130, 2017.
20. Ahmed, K., B. K. Paul, S. Chowdhury, M. S. Islam, S. Sen, M. I. Islam, S. Asaduzzaman, A. N. Bahar, and M. B. A. Miah, "Dataset on photonic crystal fiber based chemical sensor," *Data Br.*, Vol. 12, 227–233, 2017.
21. Akowuah, E. K., T. Gorman, H. Ademgil, S. Haxha, G. K. Robinson, and J. V. Oliver, "Numerical analysis of a photonic crystal fiber for biosensing applications," *IEEE J. Quantum Electron.*, Vol. 48, No. 11, 1403–1410, 2012.
22. Podder, E., R. H. Jibon, M. B. Hossain, A. Al-Mamun Bulbul, S. Biswas, and M. A. Kabir, "Alcohol sensing through photonic crystal fiber at different temperature," *Opt. Photonics J.*, Vol. 08, No. 10, 309–316, 2018.
23. Maidi, A. M., I. Yakasai, P. E. Abas, M. M. Nauman, R. A. Apong, S. Kaijage, and F. Begum, "Design and simulation of photonic crystal fiber for liquid sensing," *Photonics*, Vol. 8, No. 1, 1–14, 2021.
24. Yakasai, I., P. E. Abas, S. F. Kaijage, W. Caesarendra, and F. Begum, "Proposal for a quad-elliptical photonic crystal fiber for terahertz wave guidance and sensing chemical warfare liquids," *Photonics*, Vol. 6, No. 3, 2019.
25. Islam, S., B. Kumar, and K. Ahmed, "Liquid-infiltrated photonic crystal fiber for sensing purpose: Design and analysis," *Alexandria Eng. J.*, Vol. 57, No. 3, 1459–1466, 2018.
26. Maidi, A. M., N. Shamsuddin, W. R. Wong, S. Kaijage, and F. Begum, "Characteristics of ultrasensitive hexagonal-cored photonic crystal fiber for hazardous chemical sensing," *Photonics*, Vol. 9, No. 1, 2022.
27. Bai, X., H. Chen, and H. Yang, "Design of a circular photonic crystal fiber with square air-holes for orbital angular momentum modes transmission," *Optik (Stuttg.)*, Vol. 158, 1266–1274, 2018.
28. Maji, P. S. and P. Roy Chaudhuri, "Circular photonic crystal fibers: Numerical analysis of chromatic dispersion and losses," *ISRN Opt.*, Vol. 2013, 1–9, 2013.
29. C. Jia, H. Jia, N. Wang, J. Chai, X. Xu, Y. Lei, G. Liu, Y. Peng, and J. Xie, "Theoretical analysis of a 750-nm bandwidth hollow-core ring photonic crystal fiber with a graded structure for transporting 38 orbital angular momentum modes," *IEEE Access*, Vol. 6, 20291–20297, 2018.
30. Yakasai, I. K., P. E. Abas, S. Ali, and F. Begum, "Modelling and simulation of a porous core photonic crystal fibre for terahertz wave propagation," *Opt. Quantum Electron.*, Vol. 51, No. 4, 2019.
31. Kaijage, S. F., Z. Ouyang, and X. Jin, "Porous-core photonic crystal fiber for low loss terahertz wave guiding," *IEEE Photonics Technol. Lett.*, Vol. 25, No. 15, 1454–1457, 2013.
32. Begum, F. and P. E. Abas, "Near infrared supercontinuum generation in silica based photonic crystal fiber," *Progress In Electromagnetics Research C*, Vol. 89, 149–159, 2019.

33. Begum, F., Y. Namihira, S. M. A. Razzak, S. F. Kaijage, N. H. Hai, K. Miyagi, H. Higa, and N. Zou, "Flattened chromatic dispersion in square photonic crystal fibers with low confinement losses," *Opt. Rev.*, Vol. 16, No. 2, 54–58, 2009.
34. Kabir, M. A., M. M. Hassan, M. N. Hossain, B. K. Paul, and K. Ahmed, "Design and performance evaluation of photonic crystal fibers of supporting orbital angular momentum states in optical transmission," *Opt. Commun.*, Vol. 467, 125731, 2020.
35. Hossain, M., E. Podder, A. Adhikary, and A. Al-Mamun, "Optimized hexagonal photonic crystal fibre sensor for glucose sensing," *Adv. Res.*, Vol. 13, No. 3, 1–7, 2018.
36. Kumar, P., K. F. Fiaboe, and J. S. Roy, "Design of nonlinear photonic crystal fibers with ultra-flattened zero dispersion for supercontinuum generation," *ETRI J.*, Vol. 42, No. 2, 282–291, 2020.